Engineering peroxidase activity in myoglobin: the haem cavity structure and peroxide activation in the T67R/S92D mutant and its derivative reconstituted with protohaemin-L-histidine

Raffaella RONCONE*, Enrico MONZANI*, Monica MURTAS*, Giuseppe BATTAINI*, Andrea PENNATI*, Anna Maria SANANGELANTONI†, Simone ZUCCOTTI‡, Martino BOLOGNESI‡ and Luigi CASELLA*[1]

*Dipartimento di Chimica Generale, Università di Pavia, Via Taramelli 12, 27100 Pavia, Italy, †Dipartimento di Scienze Ambientali, Università di Parma, 43100 Parma, Italy, and ‡Dipartimento di Fisica INFM and Centro di Eccellenza per la Ricerca Biomedica, Istituto Nazionale Ricerca sul Cancro, Universita' di Genova, 16132 Genova, Italy

Protein engineering and cofactor replacement have been employed as tools to introduce/modulate peroxidase activity in sperm whale Mb (myoglobin). Based on the rationale that haem peroxidase active sites are characterized by specific charged residues, the Mb haem crevice has been modified to host a haem-distal Arg residue and a proximal Asp, yielding the T67R/S92D Mb mutant. To code extra conformational mobility around the haem, and to increase the peroxidase catalytic efficiency, the T67R/S92D Mb mutant has been subsequently reconstituted with protohaem-L-histidine methyl ester, yielding a stable derivative, T67R/S92D Mb-H. The crystal structure of T67R/S92D cyano-metMb (1.4 Å resolution; *R* factor, 0.12) highlights a regular haem-cyanide binding mode, and the role for the mutated residues in affecting the haem propionates as well as the neighbouring water structure. The conformational disorder of the haem propionate-7 is evidenced by the NMR spectrum of the mutant. Ligand-binding studies show that the iron(III) centres of T67R/S92D Mb, and especially of T67R/S92D Mb-H, exhibit higher affinity for azide and imidazole than wild-type Mb. In addition, both protein derivatives react faster than wild-type Mb with hydrogen peroxide, showing higher peroxidase-like activity towards phenolic substrates. The catalytic efficiency of T67R/S92D Mb-H in these reactions is the highest so far reported for Mb derivatives. A model for the protein–substrate interaction is deduced based on the crystal structure and on the NMR spectra of protein–phenol complexes.

Key words: hydrogen peroxide activation, myoglobin mutant, NMR spectra, peroxidase activity, X-ray structure.

INTRODUCTION

Engineering and chemical modifications of Mb (myoglobin) are extensively applied functionalization approaches aimed at introducing new enzymic activities or constructing new binding domains in the protein [1–3]. The catalytic activities that are most frequently studied with Mb derivatives are those typical of peroxidases, since the Mb haem pocket bears structural features that are more similar to those of peroxidases than those of any other protein or enzyme. Like classical peroxidases [4], Mb contains proximal (His-93) and distal (His-64) histidines [5], although it lacks other residues that play essential roles in promoting peroxidase activity. Specific key residues supporting such catalytic activity are (i) a haem-distal Arg, which favours the heterolytic cleavage of the haem-bound peroxide O–O bond through its positively charged side chain [6], (ii) a haem-distal Asn, which raises the basicity of distal histidine through a hydrogen bond to the imidazole group [7], and (iii) a haem-proximal Asp, which introduces anionic character, hence increasing the donor strength, of His-93 by hydrogen bonding to the iron-bound proximal imidazole group [8]. Although catalytic activities can be introduced into Mb through different approaches, such as random mutation [9] and cofactor modification [3], a rational approach encompasses analysis of the effect of engineering the key residues of peroxidases into the Mb haem pocket.

A main difficulty encountered in the transfer of structural features from one protein to another is related to the differences in the local folds and environment at the selected engineering sites. Correct positioning of the substituted residue is often difficult to predict even when building on a known protein structure. The studies carried out by Watanabe's group, for instance, have shown that the exact location of the distal His in Mb mutants has a strong influence on both the catalytic activity and H_2O_2-activation processes [10–12]. Therefore design of an engineered protein does not necessarily achieve a protein with increased activity.

In a previous paper, we showed that enhancement of Mb peroxidase activity on representative phenolic compounds could be achieved by introduction of a distal-site Arg residue through the Thr-67 → Arg (T67R) mutation [13]. We could also obtain an increase in the peroxidase activity of Mb by replacing the native haem with a modified protohaem [protohaemin-6(7)-L-histidine methyl ester; HM-H] containing a histidine residue bound to one of the propionic acid side chains [14]. Moreover, a S92D variant of horse heart Mb reported previously [15] showed that Asp-92 may establish a hydrogen bond with the imidazole group of the proximal His, although conformational heterogeneity of the Asp side chain prevented a clear-cut definition of such an interaction.

As a further step in the process of engineering new Mbs with structural characteristics resembling those of peroxidases, we report here the structural and functional investigation of a sperm whale Mb double mutant, T67R/S92D Mb, containing both the distal Arg and a proximal Asp residue. In addition we have analysed the binding properties and activity of the T67R/S92D Mb

Abbreviations used: Mb, myoglobin; HM-H, protohaemin-6(7)-L-histidine methyl ester; T67R/S92D Mb-H, T67R/S92D myoglobin reconstituted with HM-H; HPA, *p*-hydroxyphenyl propionic acid.

[1] To whom correspondence should be addressed (e-mail bioinorg@unipv.it).

Atomic co-ordinates and structure factors for the T67R/S92D metMbCN mutant have been deposited with the Protein Data Bank, under accession codes 1h1x and r1h1xsf, respectively.

© 2004 Biochemical Society

derivative reconstituted with the HM-H prosthetic group, which will be indicated as T67R/S92D Mb-H.

EXPERIMENTAL

Mutagenesis and protein expression and purification

Production of the T67R/S92D Mb mutant was carried out by site-directed mutagenesis of the sperm whale Mb gene with the LA PCR *in vitro* mutagenesis kit (Takara Biomedical) through PCR. A set of oligonucleotides, where the normal codon for Thr (ACC) was substituted with that for Arg (CGT) and the codon for Ser (TCG) was replaced with that of Asp (GAC), was used. The gene was then subcloned into a pET-15b vector. The T67R/S92D Mb mutant was expressed in the *Escherichia coli* BL21(DE3) strain. DNA sequencing was performed using the dye-terminator cycle-sequencing protocol and T7 Terminator and T7 Promoter primers. The dark-brown bacterial pellet containing mutated Mb was resuspended in 20 mM Tris/1 mM EDTA, pH 8.0, containing 0.5 mM dithiothreitol and 1 mM PMSF (protease inhibitor), and lysed by sonication. The crude lysate was centrifuged, filtered and loaded on to a DEAE CL-6B anion-exchange column. Fractions containing the protein were collected and the purity was checked by monitoring the absorbance ratio A_{Soret}/A_{280}, which was above 3.5. The expression of Mb yields the protein in the Fe(II)–O_2 form; the protein was then converted routinely into the metMb form by treatment with diluted H_3PO_4 to approx. pH 4, followed by several washings in phosphate buffer, pH 6.0, through a 10 kDa-cutoff filter (YM10; Amicon).

Reconstitution of T67R/S92D Mb

The reconstituted derivative T67R/S92D Mb-H was prepared following essentially the same procedure applied for reconstitution of Mb with HM-H [14]. The apo form of T67R/S92D Mb was prepared by the standard acid/2-butanone method [5]. A stoichiometric amount of HM-H complex in methanol/acetic acid (approx. 10^{-3} M) was added to the apoMb solution (5×10^{-5} M) in 10 mM phosphate buffer, pH 5.0, cooled in an ice bath. After incubation for 1 h, the solution was dialysed for 24 h against 10 mM phosphate buffer, pH 5.0 (500 ml), with slow stirring at 4 °C. A second dialysis, for an additional 24 h, against 10 mM phosphate buffer at pH 6.0, was then performed. The optical spectrum of T67R/S92D Mb-H shows a Soret band at 408 nm, with a ratio of A_{408}/A_{280} above 3.5.

Spectroscopic and binding studies

The UV/visible spectra of Mb derivatives were studied with an HP-8452A diode array spectrophotometer. Spectra were routinely taken in 0.1 M phosphate buffer, pH 6.0. The preparation of the various protein derivatives was carried out as described previously [14]. The molar absorption coefficients of the electronic bands in the absorption spectrum of T67R/S92D Mb were determined using the pyridine haemochromogen method [16]. The equilibrium constant for the binding of azide and imidazole to T67R/S92D Mb and T67R/S92D Mb-H were determined by spectrophotometric titrations as described previously [13].

^{1}H-NMR spectroscopy

^{1}H-NMR spectra were recorded at 25 °C on a Bruker AVANCE spectrometer operating at 400.13 MHz. Spectra were collected using a SUPERWEFT sequence [17], with a recycle delay of 48 ms and τ of 130 ms for aquo-metMbs and of 200 ms for metMbCN (cyano-metMb) derivatives. Proteins (approx. 1 mM) were dissolved in 50 mM phosphate buffer, pH 6.0, containing 5 % ^2H_2O for locking purposes. The cyanide adducts of T67R/S92D Mb and T67R/S92D Mb-H were obtained by addition of a small excess of KCN to solutions of the proteins. The spectra were acquired using 16384 and 8192 data points for the aquo-metMb and metMbCN derivatives, respectively, and spectral windows were set as 187 500 and 24 000 Hz, respectively. The interaction of T67R/S92D Mb with phenolic substrates was studied by recording NMR spectra of Mb solutions prepared as above and containing approx. 50 mM of the phenols. The NMR experiments were then performed under similar conditions to those described above.

Kinetic studies

The catalytic constants for the reactions between the Mb derivatives and H_2O_2 were determined with a RS-1000 model Applied Photophysics stopped-flow apparatus thermostatted at 25.0 ± 0.1 °C, coupled with an HP8452A diode array spectrophotometer. The reactions were followed by monitoring the spectral changes undergone by the protein (5.5 μM) with time (readings every 0.2 s) in the range between 390 and 440 nm, after addition of different amounts of H_2O_2 (0.1–2 mM) in 0.1 M phosphate buffer, pH 6.0. The observed first-order rate constant (k_{obs}) depends on H_2O_2 concentration. The slope of the replot of k_{obs} against H_2O_2 concentration gave the second-order catalytic constant.

The peroxidase-like activities of T67R/S92D Mb and T67R/S92D Mb-H were assayed through the steady-state kinetics of oxidation of *p*-cresol, tyramine and HPA (*p*-hydroxyphenyl propionic acid) in 0.1 M phosphate buffer, pH 6.0, at 25.0 ± 0.1 °C, following the procedures described for the catalytic reactions of wild-type and T67R Mb [13]. The conversion of the initial rate data from absorbance s^{-1} to $M^{-1} \cdot s^{-1}$ units was carried out using the difference in molar absorption coefficients at 300 nm between the dimeric products formed in the initial part of the oxidation and the phenolic substrates as described previously [13].

T67R/S92D Mb

The kinetic experiments at variable substrate concentrations were carried out under the following conditions. For the oxidation of *p*-cresol [protein] = 0.50 μM, [H_2O_2] = 13 mM and [substrate] = 0–1 mM; for the oxidation of tyramine [protein] = 1.0 μM, [H_2O_2] = 19 mM and [substrate] = 0–49 mM; for the oxidation of HPA [protein] = 1.0 μM, [H_2O_2] = 19 mM and [substrate] = 0–49 mM.

T67R/S92D Mb-H

The kinetic experiments were carried out under the following conditions. For the oxidation of *p*-cresol [protein] = 0.56 μM, [H_2O_2] = 21 mM and [substrate] = 0–1 mM; for the oxidation of tyramine [protein] = 0.56 μM, [H_2O_2] = 42 mM and [substrate] = 0–30 mM; for the oxidation of HPA [protein] = 0.56 μM, [H_2O_2] = 42 mM and [substrate] = 0–28 mM.

Structure determination

Following the final purification step, the recombinant T67R/S92D Mb was transferred in 0.05 M phosphate buffer, pH 6.0, concentrated to 43 mg/ml to ensure full oxidation and ligand saturation, and the protein was treated with $K_3Fe(CN)_6$ and KCN.

© 2004 Biochemical Society

Table 1 Statistics for the X-ray diffraction data collection and for the crystallographic refinement of T67R/S92D metMbCN

Figures in parentheses refer to the highest-resolution (1.42–1.40 Å) shell. rmsd, root mean square deviation. DPI, diffraction-component precision index.

Crystallographic parameter	Value
λ	0.933 Å
Completeness	99.1%
Reflections (total)	561 360
Unique reflections	41 560
Redundancy	13.51
I/σ overall	28.97 (3.84)
R_{merge} overall (%)	5.7% (26.4%)
Space group	P6
Cell constants	
a	90.52 Å
c	90.52 Å
c	45.13 Å
γ (deg.)	120.0°
Resolution range used in refinement	19.0–1.4 Å
R factor	12.0%
R_{free}	15.0%
rmsd bond lengths	0.015 Å
rmsd angles	1.57°
rmsd planes	0.016 Å
Cruickshank DPI	0.044 Å

Crystals of T67R/S92D metMbCN mutant were grown using the hanging-drop/vapour-diffusion technique. The 700 μl resevoir contained 3.0 M $(NH_4)_2SO_4$, 0.005 M $K_3Fe(CN)_6$, 0.005 M KCN and 0.20 M Tris/HCl, pH 9.0. The crystallization droplet contained 5 μl of the resevoir solution and 3 μl of protein solution. Rosettes of tabular crystals grew (at 294 K) in 3–4 weeks. X-ray diffraction data were collected, at 100 K, at the ESRF synchrotron radiation facility (Grenoble, France; beamline ID14-2). The cryoprotectant solution adopted was composed of 3.2 M $(NH_4)_2SO_4$, 15 % glycerol and 0.02 M Tris/HCl, pH 9.0. One crystal provided data to a maximum resolution of 1.4 Å. The T67R/S92D metMbCN crystals are isomorphus with those of wild-type recombinant Mb [18] (space group P6; unit cell constants, $a = 90.52$ Å, $b = 90.52$ Å, $c = 45.13$ Å, $\gamma = 120°$). Diffraction data were reduced and processed using the HKL package [19]. The starting structure was defined via rigid-body refinement and difference Fourier techniques, and refined in the 19.0–1.4 Å range using programs from the CCP4 suite [20]; the final R factor was 12.0 % (R_{free}, 15.0 %). The relevant data-collection and crystallographic refinement statistics are reported in Table 1. The refined model includes 1266 protein atoms, the haem, one cyanide ion, one sulphate ion and 307 water molecules. Atomic co-ordinates and structure factors for the T67R/S92D metMbCN mutant have been deposited with the Protein Data Bank, with accession codes 1h1x and r1h1xsf, respectively [21].

RESULTS

Characterization of T67R/S92D Mb and T67R/S92D Mb-H

The absorption spectra of the various ferrous and ferric derivatives of T67R/S92D Mb (Table 2) are similar to those of wild-type Mb and the T67R Mb variant [13], and bear only small changes in position or intensity of some electronic bands. Accordingly, T67R/S92D Mb also contains a six-co-ordinated, high-spin ferric centre in the metMb form, with a water molecule bound in the iron axial position, and a five-co-ordinated ferrous centre in the reduced form [22].

Table 2 Electronic spectral data for ferrous and ferric derivatives of T67R/S92D Mb and T67R/S92D Mb-H

Spectra were recorded in 0.1 M phosphate buffer, pH 6.0, at 25 °C. Absorption coefficients (in $mM^{-1} \cdot cm^{-1}$) are given in parentheses.

	Electronic spectral data (nm)	
Derivative	T67R/S92D Mb	T67R/S92D Mb-H
Fe(II)	434 (114), 574 (17), 586 (14)	434 (100), 574 (13), 582 (10.4)
Fe(II)–O_2	416 (116), 542 (12), 580 (14)	418 (110), 542 (13.5), 580 (13.4)
Fe(II)–CO	422 (170), 538 (15), 580 (15)	422 (152), 542 (15), 576 (13.5)
Fe(III)	408 (161), 500 (12), 630 (4)	408 (150), 504 (12), 632 (5)
Fe(III)–N_3^-	420 (119), 542 (16.1), 574 (14.3)	418 (110), 542 (12.0), 572 (8.9)
Fe(III)–imidazole	412 (126), 532 (15.3), 562 (12.8)	412 (122), 534 (13.3), 562 (10.8)

Reconstitution of T67R/S92D Mb with HM-H can in principle produce four isomeric protein derivatives, depending on the type of HM-H substitution and on the mode of incorporation of the cofactor into the protein [14]. The isomeric composition is clearly shown by the NMR spectra of the protein derivatives, which will be discussed below. Contrary to the reconstituted derivative obtained from Mb and HM-H, which consisted of a mixture of high-spin and low-spin forms [14], T67R/S92D Mb-H is totally high-spin, as shown by its electronic spectral features (Table 2).

Introduction of the positively charged Arg residue in the Mb distal region increases the affinity of the Fe(III) centre for small negatively charged ligands. For azide, this effect is more pronounced in the double mutant T67R/S92D Mb [$K = (9.0 \pm 0.1) \times 10^4$ M^{-1}] than in T67R Mb [$K = (6.0 \pm 0.1) \times 10^4$ M^{-1}], as compared with wild-type Mb [$K = (5.0 \pm 0.1) \times 10^4$ M^{-1}]. Additionally, the proximal mutation increases the affinity for the bulky imidazole ligand, which is significantly protonated at pH 6.0, by a factor of four relative to the distal mutant: $K = 47.0 \pm 1.2$ M^{-1} for T67R/S92D Mb as compared with 12.0 ± 0.2 M^{-1} for T67R Mb and 24.7 ± 0.7 M^{-1} for wild-type Mb [13]. The affinity for both ligands further increases in the case of T67R/S92D Mb-H, with $K = (1.50 \pm 0.01) \times 10^5$ M^{-1} for azide and $K = 89 \pm 2$ M^{-1} for imidazole.

X-ray structure

The crystal structure of the T62R/S92D metMbCN mutant, refined at 1.4 Å resolution, conforms closely to the wild-type metMbCN structure (Protein Data Bank accession code 1EBC) [18]. The root mean square deviation calculated over 147 backbone C_α atoms is 0.60 Å. As expected from analysis of the T67R/S92D Mb mutant spectral properties, the major structural features of the haem-distal and -proximal sites are conserved, the two mutations bearing essentially local reshaping of residues and solvent molecules. In particular, the T67R mutation is reflected by localization of one water molecule (W86 in Figure 1), at the distal-site entrance gate. W86 is hydrogen bonded to the guanidino group of Arg-67 (2.87 Å), at the same time being at hydrogen-bonding distance from His-64 $N_\delta 1$ (2.71 Å). Moreover, W86 can hydrogen bond the carboxylate group of the haem propionate-7 (2.86 Å), when the propionate group adopts one of the two conformations observed in the crystal structure (see Figure 1). Despite the establishment of such distal-site hydrogen-bonding network, the conformation of His-64 is little affected, and the residue is hydrogen bonded to the bound cyanide distal N atom (His-64 $N_\varepsilon 2$–N_{CN} 2.66 Å). Accordingly, the cyanide co-ordination geometry is also virtually unaffected relative to the wild-type Mb structure: the

© 2004 Biochemical Society

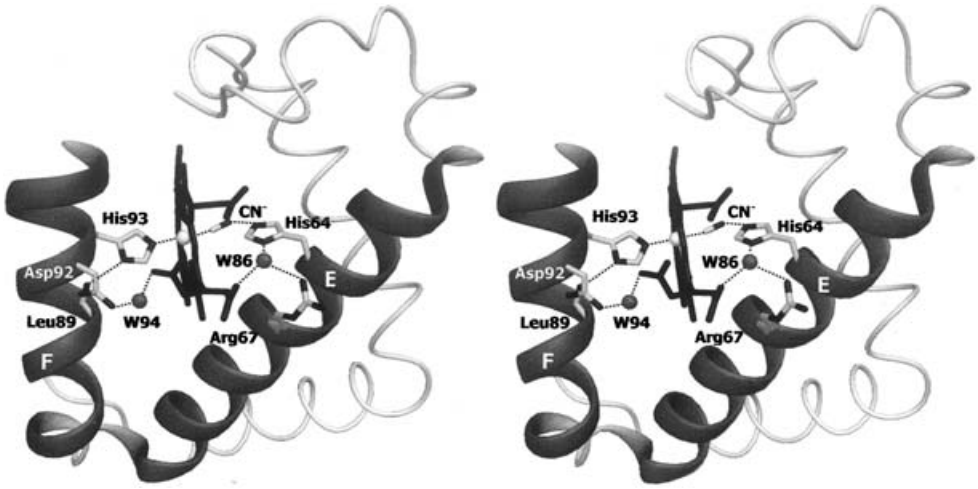

Figure 1 Structure of T67R/S92D metMbCN

Stereo view of the T67R/S92D metMbCN structure, showing details of the distal and proximal sites, where hydrogen bonds are indicated by broken lines, and key residues identified. The haem group (at the centre) is shown edge-on; the E and F helices, distal and proximal to the haem, respectively, are shown in dark grey and labelled. The rest of the globin fold is drawn as a thin backbone trace. For further details, see text [drawn with DINO Visualizing Structural Biology (2001); http://www.bioz.unibas.ch/~xray/dino].

Fe–C_{CN} co-ordination distance is 1.99 Å, and the Fe-C-N angle is 169° in the T67R/S92D mutant (these values are 2.02 Å and 166°, respectively, in wild-type metMbCN).

On the haem-proximal side, the S92D mutation is also reflected by localization of one water molecule (W94), which bridges the mutated residue and the haem propionate-7, in the second conformation observed. As a result of the residue size and of the W94 hydrogen bonds (2.74 Å to Asp-92 carboxylate, and 2.81 Å to propionate-7), the hydrogen bond between side chains connecting Ser-92 to His-93 in wild-type Mb is lost in the T67R/S92D mutant, while the His-93 $N_{\delta}1$–O Leu-89 hydrogen bond (2.93 Å) is preserved. Comparison of the wild-type and mutant Mb structures shows that the proximal His-93 imidazole ring is rotated by about 6° in relation to the altered hydrogen-bonding pattern established, while maintaining a regular co-ordination bond to the haem Fe atom (His-93 $N_{\varepsilon}2$–Fe, 2.07 Å).

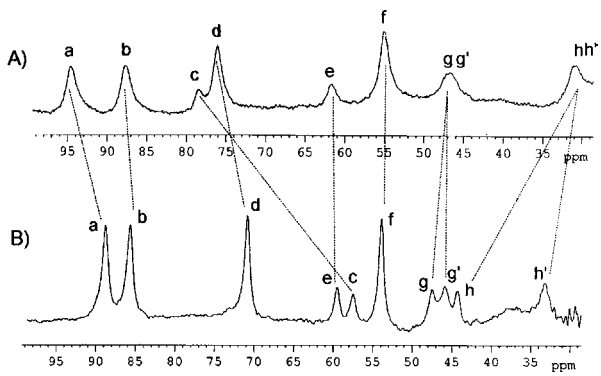

Figure 2 Proton NMR spectra of wild-type and T67R/S92D Mb

Downfield region of the 400 MHz ^{1}H-NMR spectra of wild-type Mb (**A**) and T67R/S92D Mb (**B**). The assignments of the signals labelled from a to h′ are reported in Table 3. Proteins were dissolved in 50 mM phosphate buffer, pH 6.0, containing 5 % ^2H_2O for locking purposes; spectra were recorded at 25 °C.

NMR spectra

The downfield region of the ^{1}H-NMR spectra of wild-type and T67R/S92D metMb at pH 6.0 are compared in Figure 2. The chemical shift pattern of the porphyrin methyl groups and most of the other one-proton signals are similar in both proteins. The distribution of paramagnetically shifted signals, largely due to contact interactions, is consistent with a six-co-ordinated haem iron, bearing a water molecule as axial ligand of the iron in T67R/S92D Mb. The similarity in spectral shape between the spectra of T67R/S92D Mb, wild-type Mb [23], S92P Mb and S92A Mb [24] enables unambiguous assignment of the downfield resonances as reported in Table 3. The most notable differences between the T67R/S92D and wild-type Mb spectra are the chemical shifts of the propionate-7 H_{α} signals (c and h in Figure 2), at 75.5 and 30.9 p.p.m. in wild-type, which come much closer together, at 57.5 and 44.3 p.p.m., respectively, in the double mutant. The large change in the 7-H_{α} shift, previously noted also for S92P and S92A Mb, was attributed to a reorientation of the propionate chain [24]. As shown by the X-ray data reported herein, this effect is associated with the presence of two propionate-7 conformations, which are in rapid exchange in solution.

The ^{1}H-NMR spectrum of T67R/S92D metMbCN is shown in Figure 3. The spectrum exhibits features similar, though not identical, to those of S92P and S92A metMbCN [24], and therefore a tentative partial assignment of the signals based on spectral similarities is given in Table 3. Two exchangeable resonances belonging to His-64 $N_{\varepsilon}H$ and His-93 $N_{\delta}H$ (a and c in Figure 3) are not observed in deuterated buffer. The resonances of Ile-99, which are typically upshifted for wild-type Mb [24], and also horse Mb [15], experience significantly different chemical shifts in both T67R/S92D metMbCN (k and l in Figure 3) and the cyanide adducts of other Ser-92 mutants [24] (Table 3). In contrast, the other resonances belonging to the distal and proximal residues Phe-43, His-64 and His-93 show relatively small chemical shift variations. This indicates that the relative orientation of the *z* axis of the paramagnetic anisotropy tensor has not been perturbed significantly [25,26]; thus neither the proximal nor the distal mutations affect the cyanide tilt [25]. In addition, the perturbed chemical shift of Ile-99 protons, whose hyperfine shifts are purely dipolar in origin, suggests that the rhombic magnetic axes, and

© 2004 Biochemical Society

Table 3 Proton chemical shifts (p.p.m.) for the haem and haem pocket residues of Mb mutants

Signals labelled a to h′ and a to l are shown in Figures 2 and 3 respectively.

Protein	Proton	Proton chemical shift (p.p.m.) T67R/S92D	S92P*	S92A*	Wild type*†
MetMb-H_2O					
a	8-CH_3	88.9	–‡	–‡	91.7
b	5-CH_3	85.8	–	–	84.9
c	7-H_α	57.5	–	–	75.5
d	3-CH_3	70.9	–	–	73.2
e	6-H_α	59.5	–	–	59.2
f	1-CH_3	53.9	–	–	53.2
g	4-H_α	47.6	–	–	46.4
g′	6-$H_{\alpha'}$	45.9	–	–	44.9
h	7-$H_{\alpha'}$	44.3	–	–	30.9
h′	2-H_α	33.2	–	–	31.4
MetMbCN					
a	His-64, $N_\varepsilon H$	25.1	24.1	24.5	23.7
b	5-CH_3	24.2	23.6	25.0	27.0
c	His-93, $N_\delta H$	22.4	22.5	22.3	21.1
d	Phe-43, $C_\xi H$	17.6	17.9	18.2	17.3
e	2-H_α	17.1	17.5	17.7	17.8
f	1-CH_3	16.5	16	16.4	18.6
g	Phe-43, $C_\varepsilon H$	13.3	12.8	13.2	12.6
h	His-64, $C_\delta H$		11.6	11.8	11.7
	His-93, NH	12.7	12.0	13.3	13.9
i	8-CH_3	11.0	10.7	11.0	12.9
j	His-93, $C_\beta H$		10.0	10.3	11.7
	6-Hα	10.1	10.8	9.9	9.2
k	Ile-99, $C_\delta H_3$		– 3.1	– 3.2	– 3.8
	Ile-99, $C\gamma H_3$	– 3.2	– 3.4	– 3.2	– 3.5
l	Ile-99, $C_\gamma H$	– 8.0	– 8.1	– 8.3	– 9.6

* Data from [24].
† Data from [23].
‡ Data not available from [24].

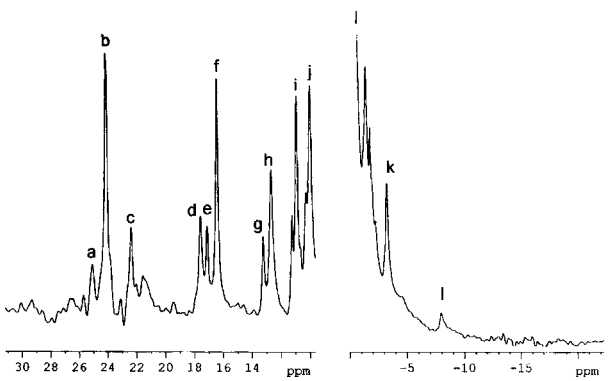

Figure 3 Proton NMR spectrum of T67R/S92D metMbCN

400 MHz ^{1}H-NMR spectrum of T67R/S92D metMbCN recorded at 25 °C. The assignment of the resonances labelled from a to l is reported in Table 3. Protein was dissolved in 50 mM phosphate buffer, pH 6.0, containing 5 % ^2H_2O for locking purposes.

therefore the His-93 imidazole ring, experience a slight rotation in the T67R/S92D Mb mutant [26–28]. The contact shifts of the methyl protons, on which the relative orientation of His-93 has a large influence [28,29], are different for T67R/S92D metMbCN. Indeed, the superposition of the haem moieties of T67R/S92D metMbCN and wild-type metMbCN shows a rotation of the His-93 imidazole amounting to about 6°.

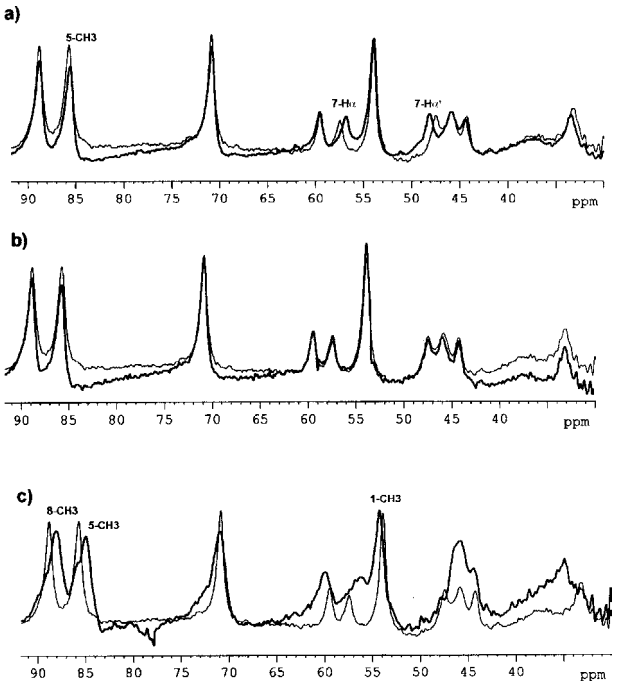

Figure 4 Proton NMR spectra of T67R/S92D metMb–phenol complexes

Downfield region of 400 MHz ^{1}H-NMR spectra of T67R/S92D metMb in the presence of saturating concentrations of (**a**) HPA, (**b**) tyramine and (**c**) *p*-cresol (bold traces) compared with the protein spectra in the absence of substrates. Protein samples were dissolved in 50 mM phosphate buffer, pH 6.0, with 5 % ^2H_2O at 25 °C.

In the presence of saturating concentrations of the phenolic substrates used in the catalytic reactions, the paramagnetic ^{1}H-NMR spectra of T67R/S92D metMb and metMbCN protein derivatives exhibit variable changes, depending on the type of substituent on the phenol ring, as reported in Figures 4 and 5. The addition of HPA produces a sizable shift in the resonance of propionate-7 of T67R/S92D metMb, but a slight shift can be detected also for the methyl group in position 5 (Figure 4a). Examination of the effect of the phenol on the low-spin cyanide derivative (Figure 5a) confirms that the signal of methyl 5 and also that of the His-64 $N_\varepsilon H$ group are perturbed. In contrast, the interaction with tyramine does not produce any evident changes in the NMR spectra of either T67R/S92D metMb or metMbCN derivatives (Figures 4b and 5b). On the other hand, the uncharged substrate *p*-cresol produces appreciable changes in several of the paramagnetic signals for both T67R/S92D metMbH_2O and metMbCN derivatives (Figures 4c and 5c). The slight shift of methyl 1 in the metMb spectrum probes the ability of this substrate to enter deeply into the haem-distal cavity. This effect is also evident in the metMbCN spectrum, where the resolution of the signals is higher.

The NMR spectrum of T67R/S92D Mb-H contains the overlap of signals due to different isomers of the protein, but confirms the absence of any contribution by low-spin forms (Figure 6a). It is interesting to note that the change induced by the haem modification in position 6/7 of the porphyrin affects mostly the resonance position of the other propionate signal, 7/6-H_α, as it occurs in the range between 55 and 70 p.p.m.. This pattern could be attributable to the possible interaction of the new histidine moiety with the proximal hydrogen bonds network that is already modified by the S92D mutation. The downfield NMR spectrum of cyanomet T67R/S92D Mb-H, which contains narrower signals, actually shows that the isomers of the reconstituted protein are three, with

© 2004 Biochemical Society

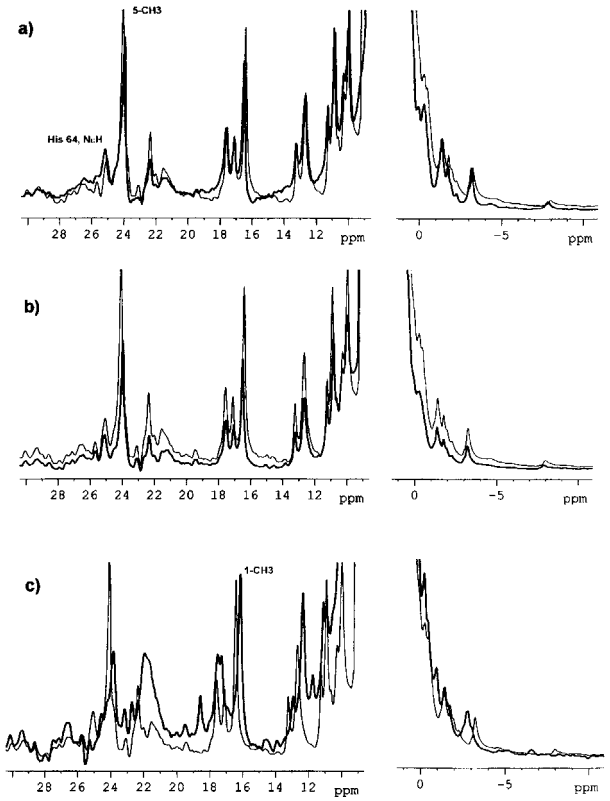

Figure 5 Proton NMR spectra of T67R/S92D metMbCN–phenol complexes

400 MHz ^{1}H-NMR spectrum of T67R/S92D metMbCN in the presence of saturating concentration of (**a**) HPA, (**b**) tyramine and (**c**) *p*-cresol (bold traces) compared with the protein spectrum in the absence of substrate. Protein samples were dissolved in 50 mM phosphate buffer, pH 6.0, with 5 % ^2H_2O, at 25 °C.

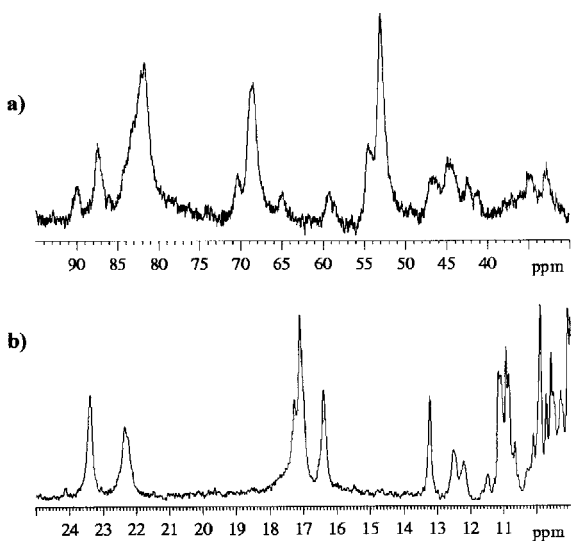

Figure 6 Proton NMR spectra of T67R/S92D metMb-H and T67R/S92D metMbCN-H

Downfield region of 400 MHz ^{1}H NMR spectra of (**a**) T67R/S92D Mb-H and (**b**) cyano-met T67R/S92D Mb-H in 50 mM phosphate buffer, pH 6.0, with 5 % ^2H_2O, at 25 °C.

one being dominant (Figure 6b). This isomer is characterized by the NMR signals at 23.4 p.p.m., attributable to the porphyrin methyl 5, and 17.1 p.p.m., attributable to methyl 1.

Table 4 Kinetic parameters for the catalytic oxidation of phenols by T67R/S92D Mb, wild-type Mb and T67R/S92D Mb-H, and H_2O_2 in 0.1 M phosphate buffer, pH 6.0, at 25 °C

Data for wild-type Mb are from [13].

Substrate	Protein	k_{cat} (s^{-1})	K_m (mM)	k_{cat}/K_m ($M^{-1} \cdot s^{-1}$)
p-Cresol	T67R/S92D Mb	–*	–*	2200 ± 200
	Wild-type Mb	–	–	4800 ± 160
	T67R/S92D Mb-H	–	–	2500 ± 100
HPA	T67R/S92D Mb	1.5 ± 0.6	20 ± 2	80 ± 6
	Wild-type Mb	1.0 ± 0.1	72 ± 5	14 ± 1
	T67R/S92D Mb-H	6.6 ± 0.3	20 ± 2	330 ± 20
Tyramine	T67R/S92D Mb	1.1 ± 0.1	40 ± 6	28 ± 2
	Wild-type Mb	0.36 ± 0.02	4 ± 1	90 ± 11
	T67R/S92D Mb-H	1.6 ± 0.1	8 ± 1	210 ± 5

* Not determinable, see text.

Kinetics

The reaction of Mb with H_2O_2 occurs initially with co-ordination of the peroxide to the iron(III) centre. Then heterolytic cleavage of the haem-bound peroxide O–O bond produces the ferryl haem species [Fe(IV) = O], coupled with a protein radical [12,30]. After quenching of the latter radical a species equivalent to compound II of peroxidases is formed. For T67R/S92D Mb and T67R/S92D Mb-H, the optical features of this species (Soret band at 422 nm) are similar to those of wild-type Mb but the rate constants for its formation (2100 ± 40 and 2100 ± 200 $M^{-1} \cdot s^{-1}$, respectively) are appreciably enhanced with respect to wild-type Mb (760 ± 10 $M^{-1} \cdot s^{-1}$) and T67R Mb (1550 ± 10 $M^{-1} \cdot s^{-1}$) under the same conditions [13].

According to the peroxidase catalytic cycle [31], the first catalytic intermediate, known as compound I, reacts in a fast step with a phenolic substrate to produce a phenoxy radical and the compound II intermediate, which is able to react with a second molecule of substrate to produce a second radical. The peroxidase-like activity of T67R/S92D Mb and T67R/S92D Mb-H was investigated using representative phenolic substrates. As described in detail for T67R Mb [13], the steady-state data can be analysed in terms of the catalytic constants reported in Table 4. With HPA and tyramine the kinetic experiments at various substrate concentrations were performed under H_2O_2-saturating conditions; with *p*-cresol, saturation of H_2O_2 could be obtained only at low (< 1 mM) substrate concentrations. Under these conditions the reaction rate depends linearly on *p*-cresol concentration; from the slope of the graph of rate against [*p*-cresol] the ratio k_{cat}/K_m could be deduced. The T67R/S92D variant shows higher reactivity towards HPA and tyramine with respect to wild-type Mb, but its activity is comparable with that of T67R. By contrast, the activity of T67R/S92D Mb-H towards these substrates is markedly increased, even with respect to HM-H-reconstituted Mb [14], as shown by both the k_{cat} and k_{cat}/K_m parameters.

DISCUSSION

We have prepared the T67R/S92D mutant of sperm whale Mb in the attempt to reproduce in the haem cavity of this protein structural features that are typically found in haem peroxidases [4]. The crystal structure analysis of the T67R/S92D metMbCN derivative shows that the Asp residue introduced in the proximal site participates in a network of hydrogen bonds centred on W94 and involving His-93 and the haem propionate-7, but is not directly hydrogen-bonded to His-93. A notable structural feature of the

© 2004 Biochemical Society

present metMbCN variant is the observation of two conformations for propionate-7, which allow the porphyrin substituent to span the proximal and distal sides of the haem crevice through hydrogen-bonding interactions with water molecules (W86 and W94), held strongly in their positions by multiple hydrogen bonds with the mutated residues and the proximal and distal histidines (Figure 1). As shown by the similarity of the spectral characteristics of T67R/S92D Mb with those of wild-type Mb, the electronic structure and co-ordination site of the haem chromophore have not been affected markedly by the double mutation. The conformational changes undergone by the propionate-7 group upon T67R/S92D replacement are signalled by marked shifts in the NMR signals of the α-methylene protons (Figure 2). The mobility of propionate-7 is apparently determined by the loss of hydrogen-bonding interaction between Ser-92 and the propionate carboxyl group in wild-type Mb [18], since NMR shifts comparable with those observed here for T67R/S92D Mb were noted previously for the S92P and S92A Mb mutants [24].

Possibly related to the increased conformational freedom of the propionate-7 side chain in T67R/S92D Mb is the successful reconstitution of this mutant with the modified HM-H cofactor. In contrast, we have not been able to obtain a stable reconstituted protein using the T67R Mb mutant. Also peculiar to T67R/S92D Mb-H is the complete absence of low-spin reconstitution isomers, characterized by a bis-histidine six-co-ordinated iron(III) centre resulting from structural rearrangements of the distal site, that were the major isomeric forms of the protein obtained upon Mb reconstitution with HM-H [14]. The presence of these low-spin forms complicated the interpretation of the ligand-binding behaviour of the reconstituted protein and of the catalytic oxidation experiments; in fact, both types of process necessarily require the preliminary displacement of the haem–Fe-bound distal histidine. Therefore, even though we expect that the loss of the protein contact involving one of the propionate substituents leads to some mobilization of the polypeptide chain upon reconstitution of the protein with HM-H, this effect is not so drastic in T67R/S92D Mb-H as it is in Mb-H [14], and the protein scaffold in the distal site is substantially maintained upon cofactor replacement.

The T67R/S92D Mb mutant and especially the reconstituted T67R/S92D Mb-H derivative exhibit enhanced binding affinity for exogenous ligands, such as azide and imidazole, with respect to wild-type Mb, and are therefore expected to similarly stabilize the binding of H_2O_2. The distal Arg-67 residue most likely contributes to the activation of the bound hydroperoxide, in the formation of ferryl Mb, through its positively charged side chain, even though its distance from the Fe atom (Figure 1) appears to be too large to enable a strong polarization of the O–O bond, as it is supposed to occur in peroxidases [6]. The role of Asp-92 is less obvious because, as shown in the X-ray structure, it interacts with the haem propionate in one conformer but is mostly free when the same propionate is involved in hydrogen bonding through W86 to His-64 and Arg-67. It is possible that, in this state, Asp-92 can interact with His-93, thereby increasing the electron-donating effect of the proximal imidazole group to the Fe(III) centre, which would result in weakening the peroxide O–O bond [8].

The NMR experiments carried out to characterize the interaction between the phenolic substrates and the T67R/S92D metMb or metMbCN derivatives (Figure 4 and 5) complement the picture emerging from the previous NMR relaxation data obtained using wild-type and T67R Mb [13]. The largest NMR shifts produced by the acidic phenol, HPA, on the protein spectrum are localized on the groups near the solvent-accessible side of the haem moiety, particularly the propionate-7 protons, which are close to the positively charged Arg residue. This mutation, therefore, drives the binding of the negatively charged phenolic compound. The K_m values for HPA are in fact much lower for both T67R and T67R/S92D Mb mutants, and also for T67R/S92D Mb-H, than for wild-type Mb (Table 4). This finding could be explained by taking into account the fact that the electrostatic interaction between Arg-67 and the carboxylate group of the haem propionate-7 reduces the contrasting effect that this negatively charged group exerts on the binding of HPA to the protein. Similar considerations, but with opposite effects, could be advanced for the binding of tyramine, whose K_m value is larger for both Arg-67 mutants than for wild-type Mb. In this case, none of the paramagnetically shifted protein signals appears to be perturbed, suggesting that this positively charged substrate apparently binds to the protein outside the haem pocket, probably via electrostatic interactions with polar residues of the protein surface.

Various contributions lead to the observed increase of peroxidase-like activity by T67R/S92D Mb and T67R/S92D Mb-H with respect to wild-type Mb. The k_{cat} values increase in the series wild-type Mb < T67R/S92D Mb < T67R/S92D Mb-H (Table 4). This parameter measures the rate of electron transfer from the phenolic substrate to the compound II-like intermediate and, for a given substrate, is ruled by two factors: the redox potential of the ferryl species and the disposition of the phenolic nucleus of the substrate relative to the haem. We can expect that introduction of the positively charged Arg residue in the distal side of Mb increases the redox potential of the ferryl species, but cannot expect a further increase in this potential upon HM-H reconstitution of the protein, since the imidazole group of the cofactor in T67R/S92D Mb-H is very likely to be outside the distal cavity. Therefore, the highest k_{cat} values observed in the T67R/S92D Mb-H-mediated catalytic reactions must be further contributed by a more favourable orientation of the phenolic ring of the bound substrate, which is likely to depend on the more relaxed haem environment in the reconstituted protein.

This interpretation is supported by the binding experiments showing increased accessibility of the iron(III) centre to the bulky imidazole ligand and by the smaller K_m value found for tyramine in the case of T67R/S92D Mb-H with respect to T67R/S92D Mb. The latter effect limits the catalytic efficiency (in terms of k_{cat}/K_m) of T67R/S92D Mb but not that of T67R/S92D Mb-H. By contrast, for the negatively charged substrate HPA the increase in k_{cat} adds favourably to the reduction in K_m, resulting in a significant increase in the catalytic efficiency of the process. The 23.6-fold increase in k_{cat}/K_m found for T67R/S92D Mb-H is the largest so far reported for mutated or reconstituted Mb derivatives [1,3,9,13,14]. For *p*-cresol, the high oxidation rate depends in part on its lower reduction potential (for the phenoxide radical/phenol couple) [32], but especially on the fact that this substrate can enter the distal cavity of the Mbs and approach closely the haem in such a way that the electron transfer is favoured. This is shown by the NMR spectra reported in the present study on T67R/S92D Mb and by the NMR relaxation experiments performed previously [13].

In conclusion, the X-ray structure of the T62R/S92D metMbCN mutant, designed to mimic active-site features present in haem peroxidases, shows local changes at the mutation sites with respect to the wild-type metMbCN structure and mobilization of the propionate-7 group as a result of rearrangements of the hydrogen-bond patterns within the haem-proximal and -distal cavities. The mutant can be reconstituted with the modified protohaem HM-H, yielding a totally high-spin derivative T67R/S92D Mb-H. Both T67R/S92D Mb and T67R/S92D Mb-H exhibit enhanced binding affinity for exogenous ligands, an increase in the peroxide-activation rate and an increase in the catalytic efficiency of peroxidative reactions carried out on representative phenolic compounds. The interaction mode of Mbs and the phenolic substrates

© 2004 Biochemical Society

also affects the efficiency of the catalytic process, and a structural model for the protein–substrate interaction has been deduced on the basis of the NMR and X-ray structural data.

We are grateful to Dr John S. Olson (Rice University, Houston, TX, U.S.A.) for providing the cDNA of sperm whale Mb, and to ESRF (Grenoble, France) for granting access to ID14. This work was supported by funds from PRIN (Progetto di Ricerca di Interesse Nazionale) of the Italian MIUR, CNR (Genomica funzionale) and ASI (I/R/294/02) grants. M.B. is grateful to Istituto G. Gaslini (Genova, Italy) and CINRO/CBA (Genova, Italy) for helpful support. R.R. thanks CIRCMSB for financial support.

REFERENCES

1 Ozaki, S., Roach, M. P., Matsui, T. and Watanabe, Y. (2001) Investigations of the roles of distal heme environment and the proximal heme iron ligand in peroxide activation by heme enzymes via molecular engineering of myoglobin. Acc. Chem. Res. **34**, 818–825

2 Watanabe, Y. (2002) Construction of heme enzymes: four approaches. Curr. Opin. Chem. Biol. **6**, 1–9

3 Hayashi, T. and Hisaeda, Y. (2002) New functionalization of myoglobin by chemical modification of heme-propionates. Acc. Chem. Res. **35**, 35–43

4 Gajhede, M., Schuller, D. J., Henriksen, A., Smith, A. T. and Poulos, T. L. (1997) Crystal structure of horseradish peroxidase C at 2.15 angstrom resolution. Nat. Struct. Biol. **4**, 1032–1038

5 Antonini, E. and Brunori, M. (1971) Hemoglobin and Myoglobin in their Reactions with Ligands, North Holland Publishing Co., Amsterdam

6 Poulos, T. L. and Kraut, J. (1980) The stereochemistry of peroxidase catalysis. J. Biol. Chem. **255**, 8199–8205

7 Nagano, S., Tanaka, M., Ishimori, K., Watanabe, Y. and Morishima, I. (1996) Catalytic roles of the distal site asparagine-histidine couple in peroxidases. Biochemistry **35**, 14251–14258

8 Anzenbacher, P., Dawson, J. H. and Kitagawa, T. (1989) Towards a unified concept of oxygen activation by heme enzymes: the role of the proximal ligand. J. Mol. Struct. **214**, 149–158

9 Wan, L., Twitchett, M. B., Eltis, L. D., Mauk, A. G. and Smith, M. (1998) *In vitro* evolution of horse heart myoglobin to increase peroxidase activity. Proc. Natl. Acad. Sci. U.S.A. **95**, 12825–12831

10 Ozaki, S., Matsui, T. and Watanabe, Y. (1996) Conversion of myoglobin into a highly stereospecific peroxygenase by the L29H/H64L mutation. J. Am. Chem. Soc. **118**, 9784–9785

11 Ozaki, S., Matsui, T. and Watanabe, Y. (1997) Conversion of myoglobin into a peroxygenase: a catalytic intermediate of sulfoxidation and epoxidation by the F43H/H64L mutant. J. Am. Chem. Soc. **119**, 6666–6667

12 Matsui, T., Ozaki, S., Liong, E., Phillips, Jr, G. N. and Watanabe, Y. (1999) Effects of the location of distal histidine in the reaction of myoglobin with hydrogen peroxide. J. Biol. Chem. **274**, 2838–2844

13 Redaelli, C., Monzani, E., Santagostini, L., Casella, L., Sanangelantoni, A. M., Pierattelli, R. and Banci, L. (2002) Characterization and peroxidase activity of a myoglobin mutant containing a distal arginine. ChemBioChem **3**, 226–233

14 Monzani, E., Gatti, A. L., Profumo, A., Casella, L. and Gullotti, M. (1997) Oxidation of phenolic compounds by lactoperoxidase. Evidence for the presence of a low potential Compound II during catalytic turnover. Biochemistry **36**, 1918–1926

15 Lloyd, E., Burk, D. L., Ferrer, J. C., Maurus, R., Doran, J., Carey, P. R., Brayer, G. D. and Mauk, A. G. (1996) Electrostatic modification of the active site of myoglobin: characterization of the proximal Ser92Asp variant. Biochemistry **35**, 11901–11912

16 Fuhrhop, J. H. and Smith, K. M. (1977) Laboratory Methods in Porphyrins and Metalloporphyrins Research, Elsevier, Amsterdam

17 Inubushi, T. and Becker, E. D. (1983) Efficient detection of paramagnetically shifted NMR resonances by optimizing the WEFT pulse sequence. J. Magn. Reson. **51**, 128–133

18 Bolognesi, M., Rosano, C., Losso, R., Borassi, A., Rizzi, M., Wittenberg, J. B., Boffi, A. and Ascenzi, P. (1999) Cyanide binding to *Lucina pectinata* hemoglobin I and to sperm whale myoglobin: an X-Ray crystallographic study. Biophys. J. **77**, 1093–1099

19 Otwinoski, Z. and Minor, W. (1997) Processing of X-ray diffraction data collected in oscillation mode. Methods Enzymol. **276**, 307–326

20 Murshudov G. N., Vagin, A. A. and Dodson, E. J. (1997) Refinement of macromolecular structures by the maximum-likelihood method. Acta Crystallogr. D **53**, 240–257

21 Berman H. M., Westbrook, J., Feng, Z., Gillang, G., Bhat, T. N. and Weisseg, M. (2000) The Protein Data Bank. Nucleic Acids. Res. **28**, 235–242

22 Springer, B. A., Sligar, S. G., Olson, J. S. and Phillips, Jr, G. N. (1994) Mechanisms of ligand recognition in myoglobin. Chem. Rev. **94**, 699–714

23 La Mar, G. N., Budd, D. L., Smith, K. M. and Langry, K. C. (1980) Nuclear magnetic resonance of high-spin ferric hemoproteins. Assignment of proton resonances in met-aquo myoglobins using deuterium-labeled hemes. J. Am. Chem. Soc. **102**, 1822–1827

24 Wu, Y., Chien, E. Y. T., Sligar, S. G. and La Mar, G. N. (1998) Influence of proximal side mutations on the molecular and electronic structure of cyanomet myoglobin: an ^{1}H NMR study. Biochemistry **37**, 6979–6990

25 Rajarathnam, K., La Mar, G. N., Chiu, M. L. and Sligar, S. G. (1992) Determination of the orientation of the magnetic axes of the cyano-metMb complexes of point mutants of myoglobin by solution ^{1}NMR: influence of His E7 → Gly and Arg CD3 → Gly substitutions. J. Am. Chem. Soc. **114**, 9048–9058

26 Emerson, S. D. and La Mar, G. N. (1990) NMR determination of the orientation of the magnetic susceptibilty tensor in cyanometmyoglobin: a new probe of steric tilt of bound ligand. Biochemistry **29**, 1556–1566

27 Shokhirev, N. V. and Walker, F. A. (1998) Co- and counterrotation of magnetic axes and axial ligands in low-spin ferriheme systems. J. Am. Chem. Soc. **120**, 981–990

28 Bertini, I., Luchinat, C. and Parigi, G. (2000) The hyperfine shifts in low spin iron(III) hemes: a ligand field analysis. Eur. J. Inorg. Chem. 2473–2480

29 Bertini, I., Luchinat, C., Parigi, G. and Walker, F. A. (1999) Heme methyl ^{1}H chemical shifts as structural parameters in some low-spin ferriheme proteins. J. Biol. Inorg. Chem. **4**, 515–519

30 Fenwick, C. W. and English, A. M. (1996) Trapping and LC-MS identification of protein radicals formed in the horse heart metmyoglobin-H_2O_2 reaction. J. Am. Chem. Soc. **118**, 12236–12237

31 Anni, H. and Yonetani, T. (1992) Mechanism of action of peroxidases. Met. Ions Biol. Syst. **28**, 219–241

32 Monzani, E., Alzuet, G., Casella, L., Redaelli, C., Bassani, C., Sanangelantoni, A. M., Gullotti, M., De Gioia, L., Santagostini, L. and Chillemi, F. (2000) Properties and reactivity of myoglobin reconstituted with chemically modified protohemin complexes. Biochemistry **39**, 9571–9582

Received 11 June 2003/14 October 2003; accepted 17 October 2003
Published as BJ Immediate Publication 17 October 2003, DOI 10.1042/BJ20030863

© 2004 Biochemical Society